INSTITUTE OF PHYSICS PUBLISHING PLASMA PHYSICS AND CONTROLLED FUSION

Plasma Phys. Control. Fusion **48** (2006) L65–L72 doi:10.1088/0741-3335/48/8/L01

LETTER TO THE EDITOR

A comparison of sawtooth oscillations in bean and oval shaped plasmas

E A Lazarus[1], F L Waelbroeck[2], T C Luce[3], M E Austin[2], K H Burrell[3], J R Ferron[3], A W Hyatt[3], T H Osborne[3], M S Chu[3], D P Brennan[4], P Gohil[3], R J Groebner[3], C L Hsieh[3], R J Jayakumar[5], L L Lao[3], J Lohr[3], M A Makowski[5], C C Petty[3], P A Politzer[3], R Prater[3], T L Rhodes[6], J T Scoville[3], E J Strait[3], A D Turnbull[3], M R Wade[3], G Wang[6], H Reimerdes[7] and C Zhang[8]

[1] Oak Ridge National Laboratory, Oak Ridge, Tennessee, USA
[2] University of Texas, Austin, Texas 78712, USA
[3] General Atomics, PO Box 85608, San Diego, California 92186-5608, USA
[4] Massachussets Institute of Technology, Cambridge, Massachusetts, USA
[5] Lawrence Livermore National Laboratory, Livermore, California, USA
[6] University of California-Los Angeles, Los Angeles, California, USA
[7] Columbia University, New York, New York, USA
[8] ASIPP, China

E-mail: lazarus@fusion.gat.com and flw@mail.utexas.edu

Received 20 February 2006
Published 11 July 2006
Online at stacks.iop.org/PPCF/48/L65

Abstract

The effect of plasma shape on sawtooth oscillations in the DIII-D tokamak plasmas is investigated by comparing discharges with cross-sections shaped like a bean and an oval. The two shapes are designed so that the Mercier instability threshold is reached when the axial safety factor is below unity for the bean and above unity for the oval cross-sections. This allows the role of interchange modes to be differentiated from that of the kink-tearing mode. The differences in the nature of the sawtooth oscillations in the bean and oval discharges are found to be determined primarily by extreme differences in the electron heat transport during the reheat. In both cases, the axial safety factor is found to be near unity following the crash.

(Some figures in this article are in colour only in the electronic version)

Sawtooth oscillations are a common phenomenon in inductively driven tokamaks whereby the heat and current in the core of the plasma are redistributed at regular intervals in time. The redistribution causes a rapid drop or crash in the central pressure, and alternates with a slow reheat. The ability to model sawtooth oscillations is important in view of their effect on ignition criteria, on the seeding of magnetic islands and on confinement of fusion products.

In his classic model for sawtooth oscillations, Kadomtsev explained the crash phase as resulting from magnetic reconnection of the core caused by growth of the resistive internal kink (RIK) mode [1]. According to the resistive magnetohydrodynamic (MHD) model, the current-driven RIK mode becomes unstable when the safety factor at the magnetic axis, q_0, drops to below unity. For circular, large aspect-ratio tokamaks the stability criterion for the RIK, $q_0 > 1$, is indistinguishable from the Mercier criterion for avoiding pressure-driven interchange instabilities near the magnetic axis [2]. In a shaped plasma these criteria can be separated. The different shapes act to modify the properties of the pressure-driven instabilities by modifying the relative length of magnetic field lines lying in regions of unfavourable magnetic curvature as well as the local shear. Pressure-driven modes are also thought to play an important role in other reconnection phenomena such as magnetic storms in the earth's magnetotail [3].

Oval and bean-shaped discharges (figure 1) were designed so as to be realizable without reconfiguring the poloidal magnetic field power supplies, allowing the shapes to be switched on successive shots in the DIII-D tokamak so as to minimize systematic measurement errors. The discharges were run in the low-confinement L-mode plasmas and were heated by a neutral beam (2.5 MW) that was needed for the measurement of the ion temperature and internal poloidal magnetic field, B_θ. The line-averaged density, $\bar{n}_e$, was kept below $4 \cdot 10^{19}\,\mathrm{cm}^{-3}$ to avoid a transition to the higher confinement H-mode in the bean. Both shapes were limited on the inner wall. Comparisons were made at similar values of $\bar{n}_e$. For the first time, the ion temperature (T_i) and poloidal flux evolution were followed in detail through the sawtooth period. Qualitative differences between the ion thermal diffusivities in the two shapes were observed. Electron heat transport was probed using the high resolution electron cyclotron emission (ECE) diagnostic along with a short diagnostic pulse of electron cyclotron heating (ECH). It was found to be dramatically different in the two shapes. The differences lead to very different evolutions of the q profiles as measured with the motional stark effect (MSE) diagnostic.

Changing the plasma shape results in several qualitative differences in the sawtooth oscillations. In the oval the sawtooth crash is a relatively mild event exhibiting a precursor oscillation but no successor oscillations. Approximately 15% of the energy inside the inversion radius is redistributed within the plasma volume with negligible loss to the limiter (the inversion radius is the radius where the slope of the sawtooth ramp changes sign). In the bean, by contrast, the sawtooth crash is a violent event. It exhibits a successor oscillation but no precursor oscillations. Approximately 30% of the pressure inside the inversion radius is expelled from the core, and about 10% of the total energy is lost from the plasma to the wall. A noteworthy feature common to both shapes is that the crash is followed after roughly one quarter of the sawtooth period by a relaxation event marked by a modest drop in T_e. The period of the bean sawtooth is approximately twice that of the oval. In both shapes fast ions are observed to extend the sawtooth period. We have tested the effect of fast ions in both shapes by replacing half the neutral beam with enough ECH to maintain similar electrical conductivity. The basic behaviour described here, distinguishing bean and oval, was unchanged.

To understand the role of the plasma shape we first describe the equilibrium reconstructions done with EFIT [4]. Figure 2 shows the safety factor profiles q at times indicated as a fraction of the sawtooth period. Note that the minimum q_0 in the bean occurs at about 2/3 the period. At the same time the total pressure inside the inversion radius stops increasing. By contrast, in the oval (figure 2(b)) there is little change in either q or the pressure during the sawtooth period. One reason for high confidence in the safety factor profile reconstructions is that we know from the correlation analysis of the ECE signal with the magnetic $n = 1$ signal that the bean sawtooth collapse is followed by an interval where a small, residual double-island

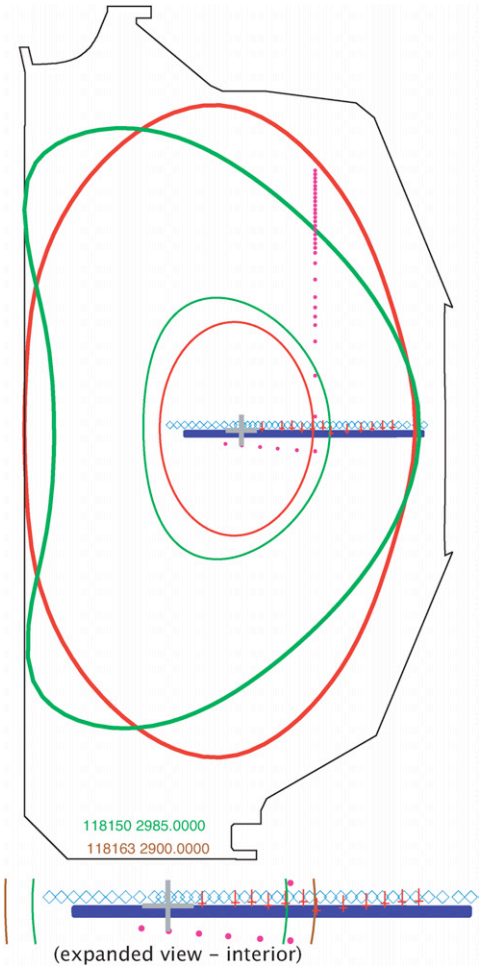

Figure 1. Plasma boundary shapes for bean and oval plasmas. The inner surfaces are at the inversion radius, r_i. Diagnostic locations are shown in an expanded view at the bottom. The solid circles (magenta) are the locations of the Thomson scattering diagnostic (n_e, T_e). The upside-down daggers (red) are the CER (T_i) locations. The solid bar (blue) is the MSE (B_Z/B_T) range of locations. Lastly, the diamonds indicate the ECE (T_e) locations.

structure exists, and its location shows good agreement with the $q = 1$ crossings shown here. The central q is near unity after every crash, in contrast to observations on other tokamaks [5–7].

Figure 3 shows the evolution of central temperatures and B_θ. In the bean the ion temperature, T_i, is near the electron temperature, T_e, but characteristically begins to roll over and decrease at about 2/3 the period; also, the rate of increase of T_e slows. The net result is that the total pressure remains essentially constant in the last third of the sawtooth period. In the oval, by contrast, the amplitude of the sawtooth excursion in T_i is much larger than that in T_e. Turning to the evolution of B_θ, we see that in the bean B_θ changes promptly at the crash. In the oval, while there is a systematic reduction in B_θ in the central region near the crash time, it is unclear whether any part of this change is synchronous with the crash in temperature.

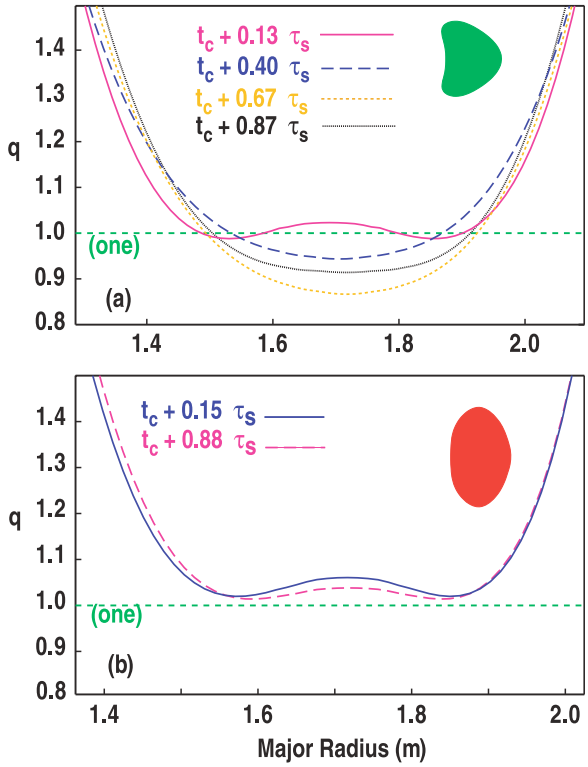

Figure 2. q profiles from equilibrium reconstruction (a) bean shape and (b) oval shape. t_c is the crash time and τ_s is the sawtooth period.

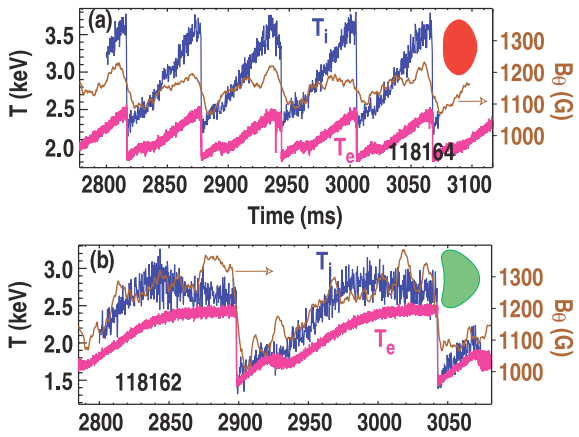

Figure 3. Evolution in time of the central electron and ion temperatures and of the poloidal magnetic field. The time resolutions for T_e, T_i and internal B_θ (from MSE) are, respectively, 5, 274 and 500 μs, for (a) the bean and (b) the oval.

We use the TRANSP code [8] to analyse the transport coefficients. For both shapes the neutral beam power is shared nearly equally between ions and electrons. Figure 4 shows the heat diffusivities volume-averaged from the axis to $\rho = 0.3$. In the oval the ion heat diffusivity, χ_i, is near the neoclassical level and ∇T_i builds rapidly after the reheat everywhere

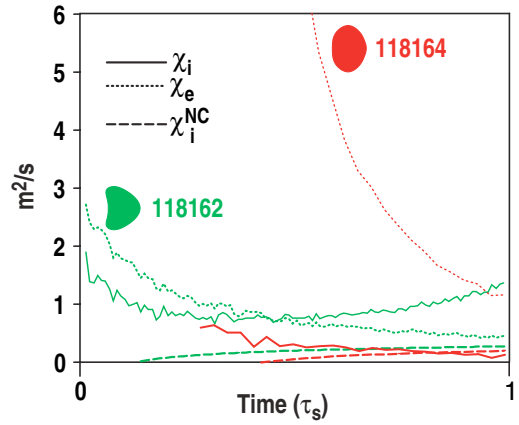

Figure 4. A comparison of electron and ion thermal diffusivities in bean and oval plasmas. The transport coefficients are volume-averaged from the axis to $\rho = 0.3$, *near* r_i, and shown as a function of the elapsed fraction of the sawtooth period. Here ρ is a flux-surface label given by the square root of the normalized toroidal flux.

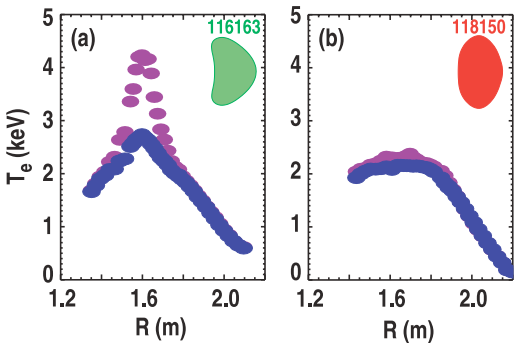

Figure 5. Response to 10 ms pulse of central ECH in middle of sawtooth ramp. The lower profiles (blue) are 1 ms before ECH and the upper profiles (violet) are 10 ms later; (*a*) bean shape with deposition centred at $\rho \approx 0.02$ and (*b*) the oval shape with deposition centred at $\rho \approx 0.06$. Note that even before the ECH there is already a substantial difference in the central ∇T_e.

within the inversion radius r_i (the radius where the slope of the sawtooth ramp changes sign). The electron heat diffusivity χ_e, however, is very large. At times earlier than shown ∇T_e is too small to allow an accurate calculation of χ_e. At the late times the magnetic axis is helical and there is significant distortion from axisymmetry. In the bean, by contrast, the initial phase of the reheat is similar for both species. The magnitude of χ_i is larger and more typical of tokamak plasmas. The increase in χ_i late in the period shows that the rollover in T_i is a result of increasing transport, rather than a change in the partitioning of the input power. The electron heat diffusivity, χ_e, is modest and very close to the 'paleoclassical' value [9] which has recently been conjectured to be the lowest possible value.

A better view of electron transport is provided by an examination of the response of T_e to a short pulse of central ECH in the middle of the reheat (figure 5). This pulse results in a 25-fold increase in the local power density to the electrons. In the bean the central T_e shows substantial increase and a strong local gradient in response to the ECH pulses, indicating good

electron confinement. In the oval there is no local response; there is a small increase in T_e distributed within the inversion radius indicating a region of good confinement outside the sawtooth region, but the central ∇T_e remains unaffected. Our observations on the difference in ∇p_e are consistent with observations on the TCV experiment of the dependence of the sawtooth on shaping [10]. In those experiments, with only ECH heating, the ions were cold and the internal B_θ was not measured, so that the equilibrium reconstructions did not allow the value of q_0 to be evaluated.

The parallel resistivity is approximately neoclassical in both shapes. The predicted evolution of the magnetic pitch angle, $\tan^{-1} B_\theta / B_T$, that results from *assuming* neoclassical resistivity differs from the values measured by the MSE diagnostic by less than the 0.1° statistical error in the measurement. In the oval, the electron temperature profile inside r_i remains very flat throughout the discharge as a consequence of the large thermal diffusivity. This results in the persistence of the flat current and q profiles throughout the sawtooth period. In the bean, by contrast, the central electron temperature rises during the ramp and the $T_e^{-3/2}$ dependence of the resistivity causes the current profile to peak. This leads to the observed evolution of the axial safety factor q_0.

The differences in the safety factor profile in the bean and oval discharges give rise to very different macroscopic stability properties and thus to very different crashes. We next describe the characteristics of the $n = 1$ mode and of the crash in both types of discharges.

The bean crash has no observable precursor. The first indication of instability is a slight, highly localized flattening of the temperature profile occuring $40\,\mu$s before the crash. The crash time itself is less than $40\,\mu$s. The profile collapses from the low field side. The crash is characterized by a large successor oscillation. This successor oscillation is dominated by the $n = 1$ toroidal harmonic. The radial profile of the phase of the wave obtained by cross-correlation analysis of the ECE with the $n = 1$ signal seen on magnetic probes is consistent with that expected for a double island structure. The crash is visible in the raw MSE signals, indicating that a significant rearrangement of the current profile is occurring. MHD stability analyses using the GATO code [11] indicate that the ideal internal kink mode is unstable during much of the sawtooth period in bean discharges. The fact that no instability is observed until the end of the ramp is thought to result from the stabilization during the ramp of both the ideal and RIK modes by the diamagnetic rotation ($\omega_{*pi} \approx \gamma_{\mathrm{MHD}}$) associated with the steep pressure gradients. The sawteeth in the bean are qualitatively consistent with the internal kink in the sense that magnetic reconnection returns the safety factor to unity during the crash. As noted by other authors, however, the Kadomtsev model must be modified to account for the stabilizing effects of diamagnetic rotation and for the acceleration of the reconnection rate due to two-fluid effects [12].

The oval-shaped plasma, by contrast, exhibits a precursor oscillation reflected in the ECE signals as an $n/m = 1/1$ mode. The precursor oscillation grows on the confinement time scale, reaching a δT_e comparable to the sawtooth height. Correlation analysis reveals a 180° phase jump on the inboard side only. Such an inboard-only phase jump is inconsistent with a magnetic island. The observed asymmetry of the precursor is characteristic of pressure-driven ideal modes, in which the changing sign of the local curvature of the magnetic field lines causes the poloidal harmonics to interfere constructively in the region of unfavorable curvature (outboard) and to interfere destructively in the region of favorable curvature (inboard). Ideal modes are thus characterized by one or more inboard phase inversions and by the absence of outboard phase inversions. Were the eigenfunction that of an internal ideal kink, no phase jumps would be observed.

The eigenfunction calculated by GATO [11] is similar to that of the quasi-interchange mode invoked by Wesson [13] to explain rapid sawtooth crashes on JET, although in the

present case the mode is saturated and evolves slowly [14]. We have verified the interpretation of the precursor as a saturated quasi-interchange mode with nonlinear MHD simulations using the NIMROD [15] code. The saturation explains the continuation of the ramp long after the ideal MHD threshold has been crossed. Until the last cycle of oscillation there is no evidence for the presence of an island. A fishbone that chirps down to the primary $n = 1$ frequency is always observed to precede the crash by just a few oscillation cycles. During the crash, the drop in the central B_θ is slow (figure 3(*b*)). The equilibrium reconstructions show that there is very little helical flux (the flux through a ribbon subtended by the magnetic axis and a $q = 1$ line) in the core, and the MSE measurements indicate that the change in B_θ during the crash is likewise very small. Thus, the observations do not allow us to discriminate between two possibilities: that the release of heat is caused by an electrostatic mechanism, or by a magnetic reconnection process in the region where the flux is compressed by the saturation of the quasi-interchange mode. The observations and stability analysis do allow us, however, to exclude the interpretation of [10], which attributed the lack of pressure peaking as well as the dependence of the sawtooth period on auxiliary heating to the linear ideal (MHD) stability properties of the oval shape.

A possible explanation for the sensitivity of transport to shaping is that shaping directly affects the properties of short wavelength pressure gradient driven modes. A difficulty with this explanation is that the interchange modes predicted by the Mercier criterion should affect both species equally. This is inconsistent with the observation of strong electron transport but good ion confinement in the oval discharges. In both shapes, the Mercier criterion, evaluated using BALOO [16], is violated over the entire sawtooth region. In the oval this violation is caused almost entirely by the ion temperature gradient, the density and electron temperature gradients being comparatively small. Ion kinetic effects presumably account for the observations by modifying the Mercier criterion so as to allow pressure gradients to be sustained [17].

In summary, changing the plasma shape so as to raise the safety factor at which the Mercier criterion is violated causes the characteristics of the sawtooth to change from kink-like to quasi-interchange-like. In all the discharges we have examined, the value of the central safety factor is close to unity after the crash. While the different magnetic shear before the crash is the proximate cause of the differences in the crash phenomenology, the magnetic shear is itself determined by the electron heat transport through the plasma conductivity. Transport is thus indirectly the cause of the observed differences.

One of us (EAL) wishes to acknowledge the many wonderful conversations with J M Greene that were the genesis of this experiment. We thank D McCune for valuable assistance with TRANSP. The work discussed in this paper was supported by the U S Department of Energy under DE-AC05-00OR22725, DE-FG03-96ER-54346, DE-FC02-04ER54698, W-7405-ENG-48, DE-FG03-01ER54615 and DE-FG02-89ER53297.

References

[1] Kadomtsev B B 1975 *Sov. J. Plasma Phys.* **1** 389
[2] Mercier C 1960 *Nucl. Fusion* **1** 47
[3] Zhu P, Bhattacharjee A and Ma Z W 2004 *J. Geophys. Res.* **109** A11211
[4] Lao L L *et al* 1985 *Nucl. Fusion* **25** 1611
[5] Soltwisch H 1988 *Rev. Sci. Instrum.* **59** 1599
[6] O'Rourke J 1991 *Plasma Phys. Control. Fusion* **33** 289
[7] Levinton F M *et al* 1993 *Phys. Fluids* B **5** 2554

[8] Hawryluk R J 1980 *Physics of Plasmas Close to Thermonuclear Conditions* ed B Coppi *et al* (Brussels: CEC) vol 1 p 19
[9] Callen J D 2005 *Phys. Rev. Lett.* **94** 055002
[10] Reimerdes H *et al* 2000 *Plasma Phys. Control. Fusion* **42** 629
[11] Bernard L C *et al* 1981 *Comput. Phys. Commun.* **24** 377
[12] Rogers B and Zakharov L 1995 *Phys. Plasmas* **2** 3420
[13] Wesson J A 1986 *Plasma Phys. Control. Fusion* **28** 243
[14] Waelbroeck F L 1989 *Phys. Fluids* B **1** 499
[15] Glasser A H *et al* 1999 *Plasma Phys. Control. Fusion* **41** A747
[16] Miller R B *et al* 1997 *Phys. Plasmas* **4** 1062
[17] Porcelli F and Rosenbluth M N 1998 *Plasma Phys. Control. Fusion* **40** 481